Journal of Hazardous Materials 168 (2009) 551–554

Contents lists available at ScienceDirect

Journal of Hazardous Materials

journal homepage: www.elsevier.com/locate/jhazmat

Short communication

Visible light-induced degradation of acetone over $SO_4^{2-}/MoO_x/MgF_2$ catalysts

Yiming He[a,b], Tianlu Sheng[a], Ying Wu[c], Jianshan Chen[a], Ruibiao Fu[a], Shengming Hu[a], Xintao Wu[a,*]

[a] State key laboratory of Structural Chemistry, Fujian Institute of Research on the Structure of Matter, Chinese Academy of Sciences, Fuzhou, Fujian 350002, China
[b] College of Mathematics, Physics and Information Engineering, Zhejiang Normal University, Jinhua 321004, China
[c] Institute of Physical Chemistry, Zhejiang Key Laboratory for Reactive Chemistry on Solid Surfaces, Zhejiang Normal University, Jinhua 321004, China

ARTICLE INFO

Article history:
Received 23 November 2008
Received in revised form 3 February 2009
Accepted 3 February 2009
Available online 13 February 2009

Keywords:
Acetone photodegradation
Photocatalyst
Sulfates
Visible light
MoO_x/MgF_2

ABSTRACT

A visible light active photodegration catalyst was prepared by doping MoO_3 into MgF_2 matrix. The addition of SO_4^{2-} into MoO_x/MgF_2 could improve the catalytic activity greatly and an acetone conversion of 96.1% under visible light was obtained on the $SO_4^{2-}/5\%\,MoO_x/MgF_2$ (SMM) catalyst. By BET, XRD, Raman, FT-IR, XPS, UV–vis technology the specific area, structure and photoadsorption ability of the catalysts were characterized. The high photocatlaytic activity of the SMM catalyst is attributed to its large specific area, the high dispersal of MoO_3 domains in MgF_2 and the inhibiting effect of MgF_2 matrix on the electron–hole pair recombination.

1. Introduction

It is well know that TiO_2 is an excellent photocatalyst that can mineralizes a large range of organic pollutants [1]. However, the band gap of TiO_2 (3.2 eV) limits its absorption to the ultraviolet region (<4%) of the solar spectrum. Hence, in order to make use of solar light source in photodegradation reaction, a visible light active photocatalyst is desired.

Coupling a large band gap semiconductor with a small band gap semiconductor is a possible way to synthesize the visible-light driven photocatalyst. Serpone et al. [2] were the first who reported the coupled catalyst. Up to now, a large variety of coupled semiconductor systems have been reported, such as CdS/TiO_2, WO_3/TiO_2, WS_2/WO_3, MoO_3/TiO_2, VO_x/MgF_2 couples [2–8]. The VO_x/MgF_2 catalyst shows the highest photon quantum efficiency (3.2% at 578 nm) under visible light [4,5]. MgF_2 with a large band gap has been proved to be a good matrix for separation of the photo electrons and holes. So, coupling MgF_2 with a small band gap semiconductor might be a new possible route to prepare the high efficient photocatalyst. The semiconductor MoO_3 has a band gap of 2.8 eV and could be active in the visible region. Lots of catalysts containing MoO_3 have been reported as photocatalysts [8–11]. However, the rapid electron–hole pair recombination makes the catalysts containing MoO_3 low activity in both ultraviolet light and visible light.

Herein, we prepared a visible light active catalyst by doping MoO_3 into MgF_2. In order to improve the photocatalytic activity of the MoO_x/MgF_2, SO_4^{2-} was induced to the coupled catalyst. It has been reported that the doping of SO_4^{2-} into TiO_2 leads to a dramatic change of the photocatalytic activity [12–14]. SO_4^{2-}/TiO_2 catalyst shows higher photocatalytic activity than unsulphated TiO_2 for a large variety of organic compounds. But for the photocatalysts without the TiO_2 phase, to our knowledge, the promotion effect of SO_4^{2-} has been seldom studied. This paper presents a new visible light active catalyst $SO_4^{2-}/MoO_x/MgF_2$ and the study of the promotion effect of SO_4^{2-}.

2. Experimental

2.1. Catalysts preparation

MoO_3 was prepared by directly decomposition of $(NH_4)_{12}Mo_7O_{27}$. MgF_2 was prepared by directly mixing $Mg(NO_3)_2$ aqueous solution and NH_4F aqueous solution with a Mg^{2+} to F^- mol ratio of 1:2, dried at 90 °C for 12 h, and then calcined in air at 350 °C for 2 h.

Preparation of $SO_4^{2-}/MoO_x/MgF_2$(SMM, n_{Mo}/n_{Mg} = 5%): 10.00 g of $Mg(NO_3)_2{\cdot}6H_2O$ was dissolved into 20 ml of H_2O to obtain solution A. 2.880 g of NH_4F was dissolved in 10 ml of H_2O to obtain solution B. 0.353 g of $(NH_4)_{12}Mo_7O_{27}$ was dissolved in 10 ml of H_2O and 3.3 ml $(NH_4)_2S$ solution (20% sulfur content) to obtain solution C (n_S/n_{Mo} = 4). Solution A was mixed with solution B and solution C under stirring to obtain a mixture. The water in the mixture was removed by a rotary evaporator to obtain a precursor solid. After dried at 90 °C for 12 h, the precursor solid was calcined in air

* Corresponding author.
E-mail address: wxt@fjirsm.ac.cn (X. Wu).

0304-3894/$ – see front matter.
doi:10.1016/j.jhazmat.2009.02.017

at 350 °C for 2 h and then cooled to room temperature to obtain the catalyst. The MoO_x/MgF_2 (MM, n_{Mo}/n_{Mg} = 5%) catalyst was prepared with the same procedure except that no $(NH_4)_2S$ solution was added.

2.2. Catalytic tests

The catalytic reaction under UV light was carried out in a quartz tube (ID 5.0 mm) reactor and two 500 W high pressure mercury lamps were used as UV light sources. When the reduction was carried out under visible light, two 400 W xenon lamps were used as visible light sources and a glass tube (ID 5.0 mm) reactor which could cut off most of the UV light was used. In each reaction, the bed length of catalyst is about 4.5 cm and the other part of the reactor was wrapped by aluminum paper to exclude the contribution of the blank reaction (Fig. 1). A thermocouple was put in the middle of the catalyst bed outside the reactor to detect the reaction temperature. The reactor tube was cooled by a fan. Because of the heat from the lamps, even we tried to cool down the reactor by the fan, the reaction temperature is still between 130 and 140 °C. Pure oxygen was used as the oxidants and acetone was used as the organic reactant. The organic substrate acetone was fed into the reactor by bubbling gas (O_2) through liquid acetone at 0 °C (cooled in a water-ice bath) to obtain the reactant mixture. The flow of mixture was controlled at 8.0 ml/min. The concentration of acetone was analyzed to be 10% by GC. The reaction products were analyzed on a GC with TCD. All the data were collected after 3 h of online reaction.

In order to rule out the thermal reaction, both the MM and SMM catalysts were tested for acetone oxidation in dark at the same reaction temperature 140 °C. The dark reaction did not show acetone degradation.

2.3. Characterizations

The XRD characterization of the catalysts was carried out on RIGAKU DMAX2500 using Cu Kα radiation (40 kV/40 mA). The specific surface areas (S_{BET}) of the catalysts were measured by nitrogen adsorption on Autosorb-1 (Quantachrome Instruments).

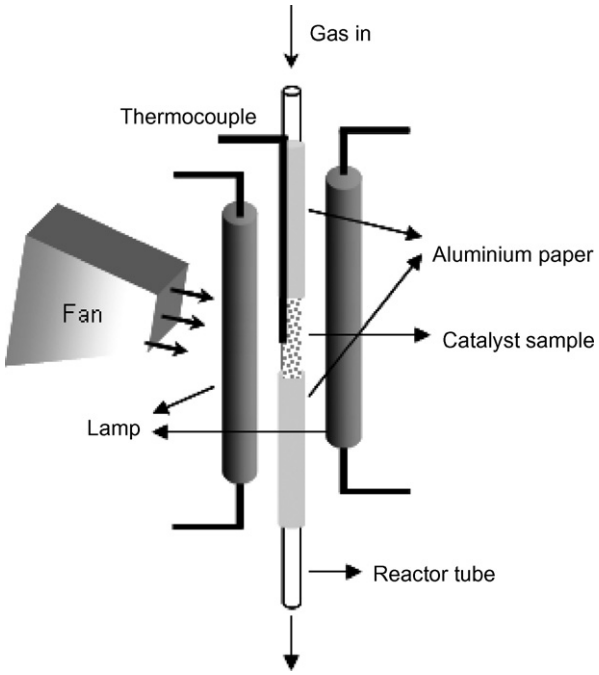

Fig. 1. The reactor system.

The Raman spectrum of the catalysts was collected on RM1000 spectrometer (Renishaw) with an Ar ion laser (514.5 nm) as excitation source. The FT-IR spectrum of the catalysts was recorded on PerkinElmer Magna 750 with a resolution of 4 cm^{-1}. The UV–vis spectrum of the catalysts was recorded on PerkinElmer Lambda900 equipped with an integrating sphere.

3. Results and discussions

3.1. Photocatalytic activity of the catalysts

The P25(TiO_2 Degussa), MgF_2, MoO_3, MM and SMM catalysts were tested in photodegradation reaction of acetone. The results are listed in Table 1. Under UV light, P25 has high activity for acetone degradation. An acetone conversion of 99.1% was obtained. MgF_2 and MoO_3 have low activity for acetone degradation. Under visible light, MgF_2 is not active, but P25 and MoO_3 showed low activity. The MM catalyst is more active than both MgF_2 and MoO_3 under both ultraviolet light and visible light. Clearly, the doping of MoO_3 in MgF_2 created a new active photodegration catalyst. The SMM catalyst shows much higher photocatalytic activity than the MM catalyst. An acetone conversion of 97.6% under ultraviolet light and an acetone conversion of 96.1% under visible light were obtained. It is obvious that the doping of SO_4^{2-} into the MM catalyst promoted the photocatalytic activity greatly. In the photodegradation of acetone, the main products are CO_2, CO, and H_2O. The similar product distribution was observed on the MM and SMM catalysts.

3.2. Characterization of the catalysts

The specific surface areas of MoO_3, MgF_2, MM and SMM are 19, 40, 110 and 150 m^2/g, respectively. An increase of the specific surface area is observed from MgF_2, MM to SMM. It is consistent with the change in catalytic activity of catalysts. Hence, the influence of specific surface area on catalytic activity might be one important factor.

The XRD patterns of the MgF_2, MM and SMM catalysts are listed in Fig. 2. MgF_2 shows several strong diffraction peaks at 2θ = 27.2°, 35.2°, 40.4°, 43.7°, 53.4°, 56.2° (JCPDS41-1443). The same diffraction peaks are also observed in the patterns of the MM and SMM catalysts and no peaks corresponding to Mo oxides phase is observed. It means that the doped MoO_3 is dispersed in the MgF_2 matrix. Meanwhile, the dispersed Mo oxides also decrease the particle size of MgF_2. As shown in Fig. 2, compared with pure MgF_2 the peak intensity of the MgF_2 on MM catalyst decreases greatly and the FWHM at 2θ = 27.2° increases from 0.33 to 0.90. On SMM catalyst, the FWHM at 2θ = 27.2° increases to 1.26. By Scherrer Formula ($d = 0.89\lambda/\beta\cos\theta$) the average crystalline sizes of MgF_2 could be calculated. The average particle sizes of the MgF_2, MM and SMM catalysts are about 25, 9.0, 6.4 nm, respectively.

Table 1
Catalytic performance of catalysts in photodegradation reaction of acetone under UV and visible light.

Light	Catalysts	Conv. (%)	Sel. (CO_2) (%)	Sel. (CO) (%)	Sel.[a] (others) (%)
UV	TiO_2	99.1	91.8	8.2	0
	MgF_2	10.7	78.5	18.6	2.9
	MoO_3	5.2	85.6	8.2	6.2
	MM	46.8	73.2	20.0	6.8
	SMM	97.6	72.8	26.8	0.4
Visible	TiO_2	14.8	90.6	9.4	0
	MgF_2	–	–	–	–
	MoO_3	6.0	81.2	13.2	5.6
	MM	42.6	71.2	23.6	5.2
	SMM	96.1	74.5	25.1	0.4

[a] *Note*: acetol (CH_3COCH_2OH) + CH_2CHO.

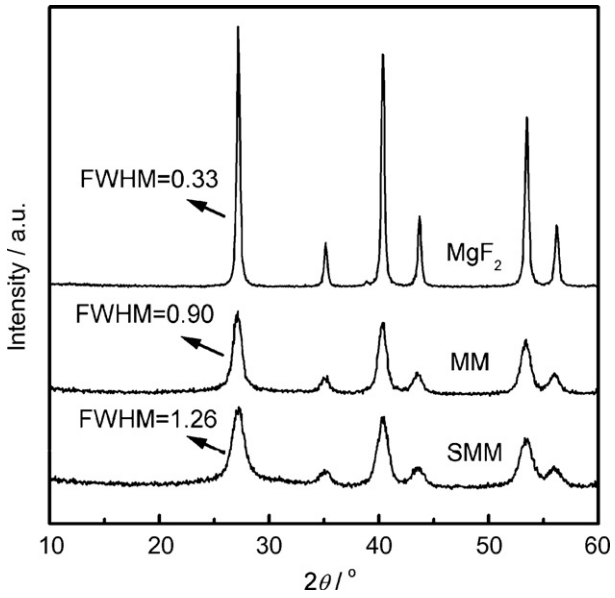

Fig. 2. XRD patterns of MgF_2, MM and SMM catalysts.

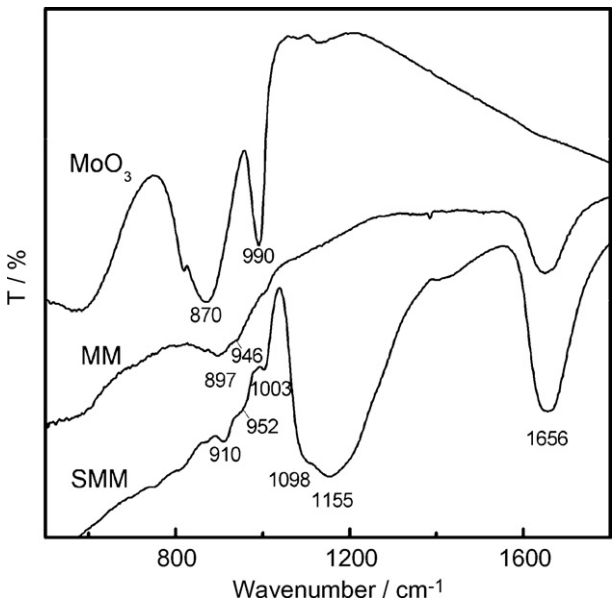

Fig. 4. FT-IR spectra of MoO_3, MM and SMM catalysts.

Fig. 3 shows the Raman spectra of the MM and SMM catalysts. MgF_2 does not have Raman band between 200 and 1200 cm^{-1}. As shown in Fig. 3, the absence of bands at 819 and 995 cm^{-1} for all the catalysts indicates the absence of MoO_3 crystallites [15]. This is consistent with the result of the XRD experiment. Moreover, a broad band in the range 800–1000 cm^{-1} is observed in Fig. 3. For the MM catalyst the maximum is at 948 cm^{-1}. While for SMM catalyst the band is weakened, with an additional strong signal at 875 cm^{-1}. As reported in literature [15], the Raman bands around 854 cm^{-1} is assigned to isolated molybdate species, while the band around 950 cm^{-1} is assigned to octahedral polymolybdate species. Obviously, the dispersion of Mo oxide in SMM catalyst is higher than that in MM catalyst.

The FT-IR spectra of the MM, SMM catalysts and pure MoO_3 are shown in Fig. 4. The spectrum of MoO_3 shows two bands at 870 and 990 cm^{-1} corresponding to vibrations of Mo=O and Mo–O–Mo, respectively [16]. For the MM catalyst one strong band is observed at 1656 cm^{-1}, which could be assigned to the absorbed H_2O species. Besides, three bands which are very weak and not well resolved are also observed at 897, 946 and 1003 cm^{-1}. Based on the literature reported [16,17], the bands at 897 and 1003 cm^{-1} could be assigned to the isolated molybdate species in which Mo is tetrahedrally coordinated, while the bands at 946 cm^{-1} could be assigned to the polymolybdate species. It is consistent with the result of Raman experiment. The difference in the phase content might be noted. Based on the intensity of the bands, it is easy to conclude that the polymolybdate species does not show much higher content than the isolated molybdate species in the FT-IR spectrum like that in the Raman spectrum. It might due to the difference of the two methods. As we know, the Raman method investigates the surface structure of the catalyst, while the FT-IR method surveys the bulk phase structure. The spectrum of the SMM catalyst is similar with that of the MM catalyst except for the two intensive bands at 1098 and 1155 cm^{-1} which are assigned to SO_4^{2-} species [12]. This assignment is confirmed by the results of XPS experiment (Fig. 5).

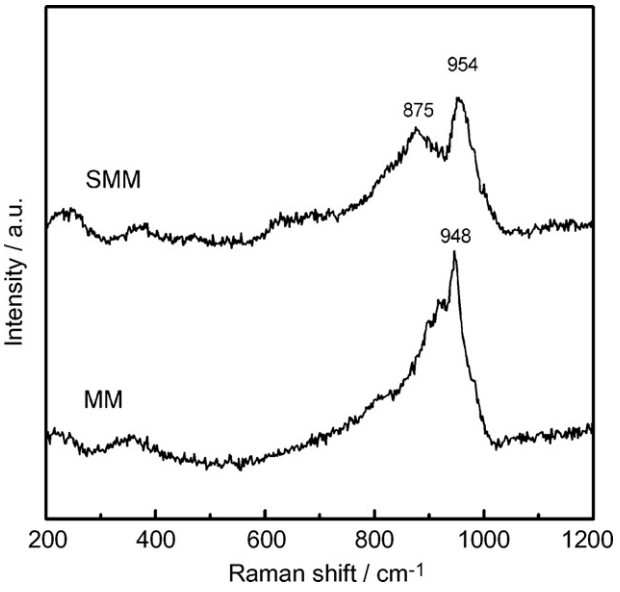

Fig. 3. Raman spectra of MM and SMM catalysts.

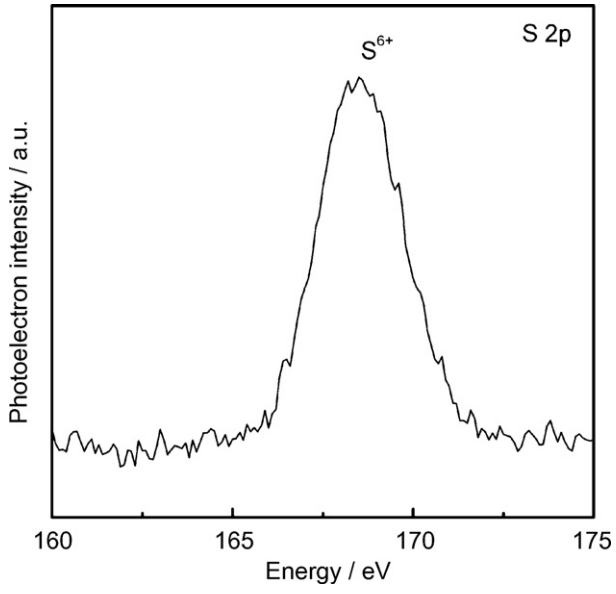

Fig. 5. S2p XPS spectra of SMM catalyst.

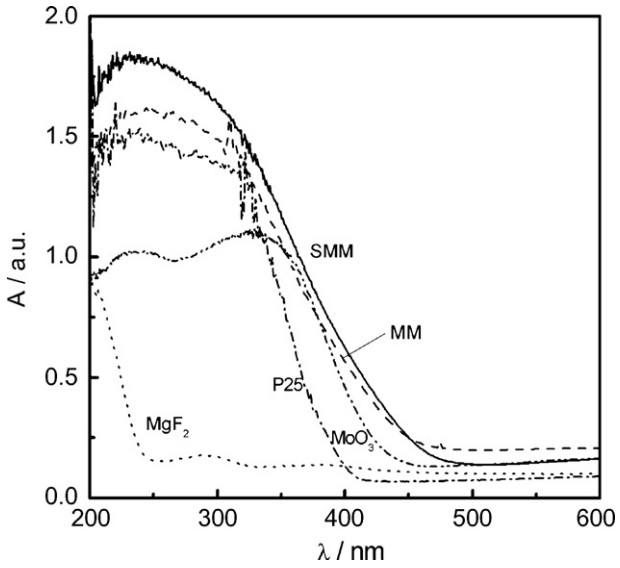

Fig. 6. UV–vis spectra of catalysts.

As shown in Fig. 6, the S2p XPS spectra has only one peak located at 168.5 eV, which is related with S^{6+} (SO_4^{2-}) [18].

Fig. 6 shows the UV diffuse-reflectance spectra of the MgF_2, MoO_3, P25, MM and SMM catalysts. Pure MgF_2 absorbs UV light (<250 nm), but not sensitive in visible light. Comparing with P25, both the MM and SMM catalysts show strong absorption in visible light region (<450 nm). It could be attributed to the MoO_x domains in the MgF_2 matrix. The UV–vis characterization is consistent with the catalytic activity testing results (MM and SMM is active under visible light).

3.3. Discussions

In the current case, MM catalyst was prepared by doping MoO_3 into MgF_2 and shows activity in visible light for acetone degradation. The structure characterizations show the doped Mo oxide is dispersed in the MgF_2 matrix. These MoO_x species, which have almost the same band gap as that of bulk MoO_3, are the active sites of catalysts. In this case, if electrons were excited from one spot of MoO_x to the other one, holes could be left behind. The isolator MgF_2 could retard the recombination of the electrons and holes. Electron–holes pairs generated in this way should have long lifetimes, which is necessary for photochemical reactions.

The foreign species such as SO_4^{2-} are often induced to TiO_2 contained catalysts to improve its photocatalytic activity [12–14]. In the present paper, sulfates are also induced to the MM catalyst and the SMM catalyst exhibited stronger photocatalytic activity than the MM catalyst. It is plausible that the stronger photoactivity of the SMM catalyst results from two factors.

The first factor is that the introduction of SO_4^{2-} can promote the specific surface area of the catalyst. The SMM catalyst has larger specific surface area than the MM catalyst. It could promote the adsorption of organic substrates on the surface of catalyst and consequently enhance the photocatalytic activity in acetone oxidation. The second factor is that the introduction of SO_4^{2-} can prolong the life of the electron–hole pairs. The Raman characterizations show the doping of SO_4^{2-} could promote the dispersal of Mo oxide in MgF_2 matrix. That means the MoO_x in the SMM catalyst has smaller particle size than that in the MM catalyst. In large MoO_3 particles, the volume recombination of the charge-carriers is the dominant process, and can be reduced by a decrease in particle size. This decrease also leads to an increase in the interfacial charge-carrier transfer rates. Thus, the isolator MgF_2 matrix could retard the recombination of the electrons and holes more effectively. So, doping SO_4^{2-} into MM catalyst decreased the particle size of MoO_x and prolonged the life of the electron–hole pairs. It makes the SMM catalyst show stronger photocatalytic activity than the MM catalyst. Besides, the change of acidity due to the addition of SO_4^{2-} might be the possible reason [13,14]. But it needs to be proved and the subsequent research is on going.

4. Conclusions

In summary, a new coupled catalyst MoO_x/MgF_2 (MM) was synthesized from the aqueous of solutions of $(NH_4)_{12}Mo_7O_{27}$, $Mg(NO_3)_2$ and NH_4F. 43.0% acetone conversion was obtained in the visible light. The high photodegradation of the MM catalyst is attributed to the inhibiting effect of MgF_2 matrix on the electron–hole pairs. The doping of SO_4^{2-} into MoO_x/MgF_2 catalyst could improve the catalytic activity greatly. It is owe to that SO_4^{2-} promote the dispersal of MoO_x domains in MgF_2 matrix and the MgF_2 could separate the electron–hole pairs more effectively. Besides, the increased specific surface area might be another reason for the higher catalytic activity.

Acknowledgements

This work was supported by grants from the 973 Program (2007CB815301 and 2006CB932904), the National Science Foundation of China (20333070, 20673118, 20871114), the Science Foundation of CAS (KJCX2-YW-M05) and of Fujian Province (2006L2005, 2007F3118).

References

[1] A. Fujishima, T.N. Rao, D.A. Tryk, Titanium dioxide photocatalysis, J. Photochem. Photobiol. C: Photochem. Rev. 1 (2000) 1–21.
[2] N. Serpone, E. Borgarello, M. Gratzel, Visible light induced generation of hydrogen from H_2S in mixed semiconductor dispersion: Improved efficency through inter-particle electron transfer, J. Chem. Soc. Chem. Commun. (1984) 342–344.
[3] J. Zhong, J. Wang, L. Tao, M. Gong, Z. Liu, Y. Chen, Photocatalytic degradation of gaseous benzene over TiO_2/Sr_2CeO_4: Prepartion and photocatalytic behavior of TiO_2/Sr_2CeO_4, J. Hazard. Mater. 140 (2007) 200–204.
[4] F. Chen, T.H. Wu, X.P. Zhou, The photodegradation of acetone over VO_x/MgF_2 catalysts, Catal. Commun. 9 (2008) 1698–1703.
[5] J. Wang, F. Chen, X.P. Zhou, Photocatalytic degradation of acetone over a V_2O_5/LaF_3 catalyst under visible light, J. Phys. Chem. C 112 (2008) 9723–9729.
[6] F. Chen, J. Wang, J.Q. Xu, X.P. Zhou, Visible light photodegradation of organic compounds over V_2O_5/MgF_2 catalyst, Appl. Catal. A: Gen. 348 (2008) 54–59.
[7] S. Hotchandani, P.V. Kamat, Charge-transfer processes in coupled semiconductor systems: photochemistry and photoelectrochemistry of the colloidal CdS-ZnO system, J. Phys. Chem. 96 (1992) 6834–6839.
[8] J. Papp, S. Soled, K. Dwight, A. Wold, Surface acidity and photocatalytic activity of TiO_2, WO_3/TiO_2, and MoO_3/TiO_2 photocatalysts, Chem. Mater. 6 (1994) 496–500.
[9] V. Zakharenko, Photoinduced heterogeneous processes on chemical phase components of solid tropospheric aerosols, Top. Catal. 35 (2005) 231–236.
[10] M. Miyauchi, A. Nakajima, T. Watanabe, K. Hashimoto, Photocatalysis and photoinduced hydrophilicity of various metal oxide thin films, Chem. Mater. 14 (2002) 2812–2816.
[11] T. He, Y. Ma, Y. Cao, P. Jiang, X. Zhang, W. Yang, J. Yao, Enhancement effect of gold nanoparticles on the UV-light photochromism of molybdenum trioxide thin films, Langmuir 17 (2001) 8024–8027.
[12] E. Barraud, F. Bosc, D. Edwards, N. Keller, V. Keller, Gas phase photocatalytic removal of toluene effluents on sulfated titania, J. Catal. 235 (2005) 318–326.
[13] X. Fu, Z. Ding, W. Su, D. Li, Structure of titania-based solid superacids and their properties for photocatalytic oxidation, Chin. J. Catal. 20 (1999) 321–323.
[14] G. Colon, M.C. Hidalgo, J.A. Navio, Photcatalytic behaviour of sulphated TiO_2 for phenol degradation, Appl. Catal. B 45 (2003) 39–50.
[15] C.C. Willianms, J.G. Ekerdt, J.M. Jehng, F.D. Hardcastle, A.M. Turek, I.E. Wachs, A Ramen and ultraviolet diffuse reflectance spectroscopic investigation of silica-supported molybdenum oxide, J. Phys. Chem. 95 (1991) 8781–8791.
[16] J. Haber, M. Wojciechowska, Surface structure and catalytic properties of the MoO_3-MgF_2 system, J. Catal. 110 (1988) 23–26.
[17] M. Henker, K.P. Wendlandt, Structure of MoO_3/Al_2O_3-SiO_2 catalysts, Appl. Catal. 69 (1991) 205–220.
[18] V. Yufit, D. Golodnitsky, L. Burstein, M. Nathan, E. Peled, X-ray photoelectron spectroscopy and time-of-flight secondary ion mass spectroscopy studies of electrodeposited molybdenum oxysulfide cathodes for lithium and lithium-ion microbatteries, J. Solid State Electrochem. 12 (2008) 273–285.